Solid-State Electronics 114 (2015) 76–79

Contents lists available at ScienceDirect

Solid-State Electronics

journal homepage: www.elsevier.com/locate/sse

A bottom-gate silicon nanowire field-effect transistor with functionalized palladium nanoparticles for hydrogen gas sensors

Bongsik Choi [1], Jae-Hyuk Ahn [1], Jieun Lee, Jinsu Yoon, Juhee Lee, Minsu Jeon, Dong Myong Kim, Dae Hwan Kim, Inkyu Park *, Sung-Jin Choi *

Mobile Sensor and IT Convergence (MOSAIC) Center, KAIST, Daejeon 305-701, South Korea
School of Electrical Engineering, Kookmin University, 861-1 Jeongneung-dong, Seongbuk-gu, Seoul 136-702, South Korea

ARTICLE INFO

Article history:
Received 3 April 2015
Received in revised form 29 July 2015
Accepted 30 July 2015

Keywords:
Hydrogen
Gas sensor
Coupling effect
Silicon nanowire
Palladium nanoparticle
TCAD

ABSTRACT

The highly sensitive operation of a bottom-gate silicon nanowire (SiNW) field-effect transistor (FET)-based hydrogen (H_2) sensor is demonstrated by controlling the working regime of the sensor. It is observed that the deposition of palladium (Pd) nanoparticles on the SiNW surface for the selective absorption of H_2 can result in a significant enhancement of the electrostatic properties, such as the subthreshold swing and on-current, of the SiNW FET-based H_2 sensor. By comparing the experimental results with the numerical simulation, we conclude that the improvement of the electrostatic properties of the sensor is due to the coupling effect between the electrostatic potentials in the Pd nanoparticle and bottom gate. Based on these results, highly sensitive detection of H_2 gas could be achieved in the subthreshold regime where the gating effect induced by absorbed H_2 gas is the most effective.

1. Introduction

Silicon nanowires (SiNWs) are being actively explored for various sensor applications, such as pH sensors [1,2], biosensors [1–3], vapor sensors [4], and gas sensors [5–7], because of the high sensitivity resulting from their high surface/volume ratio. In addition, the reason for SiNWs being preferable is that they are readily compatible with the existing semiconductor processing technologies as they have easy control of electrical properties, facile surface functionalization with chemical linkers to molecules and mechanical and chemical robustness for various field of usage [2,8]. The typical structure of SiNW sensors is based on a bottom-gate field-effect transistor (FET) capable of converting chemical interaction into electrical signals [1,5,6]. The carrier density in the channel of SiNW sensors is generally modulated through the electrostatic potential applied to the bottom gate to enhance the sensitivity by controlling the working regime to the subthreshold regime, in which a maximal sensitivity can be achieved [9]. Therefore, the exposed SiNW channel surface of bottom-gate SiNW FET sensors is employed for the detection of various biological and chemical species according to the functionalization of the SiNW surface [1,5].

Recently, hydrogen (H_2) sensors have been developed for a wide range of industrial applications, such as hydrogenation, petroleum refining processes, and hydrogen cooling systems [10,11]. Moreover, because H_2 has been considered to be a strong candidate as a future fuel and energy carrier, the utilization of H_2 sensors in the fuel cell applications, including leakage tests and fuel monitoring, has received increased attention [10,11]. In response to these demands, SiNW FET-based H_2 sensors are being developed since they can be easily fabricated by well-developed complementary metal-oxide-semiconductor (CMOS) compatible processes and their electrical properties can be easily tuned by doping [11]. However, because pristine SiNWs do not show appreciable sensitivity to H_2 [11], the surfaces in SiNW FET sensors should be functionalized with catalytic layers such as palladium (Pd) nanoparticles for the selective absorption of H_2 [5,11]. Therefore, a detailed investigation of the effect of Pd nanoparticles on the electrical properties of SiNW FET-based H_2 sensors is required to understand and optimize the device sensitivity, but insufficient studies have been performed to date. In addition, this type of investigation would be important in predicting the electrostatics of SiNW FET-based sensors for the detection of various gases in which diverse metal nanoparticles are used as catalysts.

* Corresponding authors. Tel.: +82 42 350 3233; fax: +82 42 350 3210 (I. Park). Tel.: +82 2 910 5543; fax: +82 2 910 4449 (S.-J. Choi).
E-mail addresses: inkyu@kaist.ac.kr (I. Park), sjchoiee@kookmin.ac.kr (S.-J. Choi).
[1] Contributed equally to this work.

http://dx.doi.org/10.1016/j.sse.2015.07.012
0038-1101/

In this study, therefore, we conducted an in-depth analysis of the electrostatics of a SiNW FET-based H_2 sensor functionalized with Pd nanoparticles. Importantly, it was observed that the electrostatic potential of Pd nanoparticles functionalized on the surface of a SiNW could be coupled to that of the bottom gate of the SiNW FET-based H_2 sensor, resulting in a significant enhancement in the electrical properties of the sensor. Based on these results, the highly sensitive detection of H_2 gas could be achieved by adjusting the bottom-gate potential to control the working regime of the sensor to the subthreshold regime.

2. Device structure and *I–V* characteristics

A schematic of the SiNW FET-based H_2 sensor examined in this study is shown in Fig. 1(a). Detailed information regarding the fabrication of a bottom-gate SiNW FET was presented in our previous work [12]. The phosphorous doped n-type SiNW (2×10^{18} cm^{-3}) was fabricated on a 6″ silicon-on-insulator (SOI) wafer using conventional CMOS technology. The boron doped p-type substrate underneath the 375 nm thick buried oxide in SOI wafer was used as a bottom gate. For the selective and sensitive detection of H_2 gas with the bottom-gate SiNW FET, the SiNW surface was functionalized with Pd nanoparticles by depositing a very thin Pd film (thickness ~ 1 nm) using an electron beam evaporator. It is known that the deposition of a very thin metal film, which is deposited on a silicon oxide surface, will be formed in the form of nanoparticles instead of a continuous thin film because the metal atoms tend to agglomerate due to the low surface energy of the oxide (the native oxide in our case) [13]. Fig. 1(b) shows the scanning electron microscopy (SEM) images of the Pd nanoparticles deposited on the SiNW with the width (W_{NW}) of 70 nm, the length (L_{NW}) of 10 μm, and the height of 80 nm.

The transfer characteristics of the SiNW FET-based H_2 sensor with and without Pd nanoparticles on the SiNW surface were measured using an Agilent 4156C in an ambient condition (Fig. 2(a)). To avoid device-to-device variations, the same SiNW FET was characterized before and after the deposition of Pd layer. The SiNW FET without Pd nanoparticles showed a large subthreshold swing (SS) of 2.02 V/dec and a low on-current (I_{ON}) of 82 nA because the gate control of the device was weak due to the thick gate dielectric layer in the bottom-gate FET structure (375 nm). Herein, I_{ON} is defined as the drain current (I_{DS}) at the overdrive voltage, 15 V, and the overdrive voltage is defined as V_{BG}–V_T, where the V_{BG} is the bottom gate voltage and the threshold voltage (V_T) is defined by the current constant method (0.2 nA). Interestingly, we observed that the presence of Pd nanoparticles on the SiNW could significantly improve the transfer characteristics of the sensor. After the deposition of Pd nanoparticles, the SiNW FET showed significant enhancements in I_{ON} and SS from 82 to 329.20 nA and from 2.02 to 0.34 V/dec, respectively. It should be noted that this finding is in contrast to previously reported results for H_2 sensors featuring a two-terminal SiNW structure [5]. For two-terminal SiNW H_2 sensors, it has been observed that I_{ON} tends to decrease after the deposition of Pd nanoparticles, which can be explained by the electron depletion at the Pd nanoparticle–SiNW interface due to the high work function of Pd nanoparticles [5]. However, our results show the opposite trend, i.e., an increase in I_{ON} and a steeper SS, indicating that the gate control over the SiNW channel could be improved via a coupling effect between the bottom gate and floating Pd nanoparticles. Moreover, the enhancement in the electrical properties became more prominent as W_{NW} was decreased, as shown in Fig. 2(b). Similar results have been observed for SiNW biosensors in which the presence of an electrolyte in the SiNW results in a significant enhancement in the transfer characteristics of bottom-gate SiNW FETs due to a coupling effect between the electrostatic potentials in the electrolyte and bottom gate [14,15].

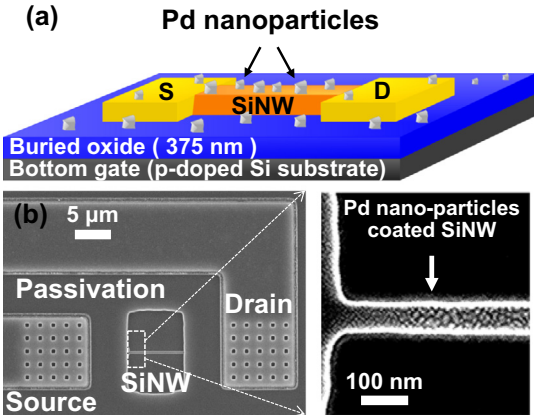

Fig. 1. (a) Schematic of a SiNW FET with a bottom-gate structure for H_2 sensing. For the detection of H_2, Pd nanoparticles were deposited on the surface of the SiNW. (b) SEM images of the fabricated device with deposited Pd nanoparticles.

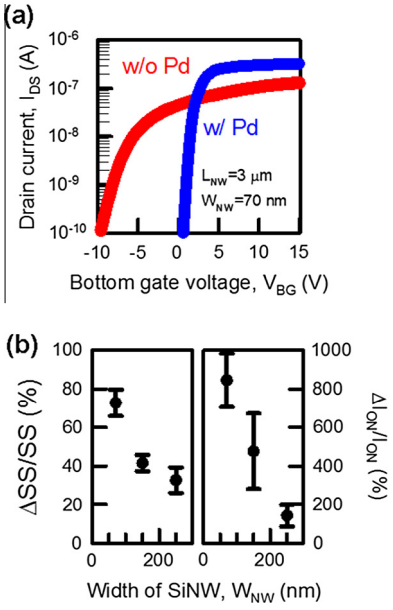

Fig. 2. Electrostatic characteristics of a SiNW FET sensor functionalized with (w/) and without (w/o) deposited Pd nanoparticles. (a) The I_{DS}–V_{BG} characteristics of the sensors w/ and w/o Pd nanoparticles at V_{DS} = 50 mV. (b) Variation in ΔSS/SS and $\Delta I_{ON}/I_{ON}$ as a function of W_{NW}. ΔSS and ΔI_{ON} are defined as the differences in the respective characteristics between the sensors w/ and w/o Pd nanoparticles.

3. Simulation result and discussion

In fact, the direct measurement of gate capacitance is the best way to investigate the enhanced gate control afforded by Pd nanoparticles, but it is difficult to measure the extremely low gate capacitance at the aF-fF level because it is shadowed by a large background parasitic capacitance [16]. Therefore, a 3D TCAD simulation was performed in order to confirm the effect of Pd nanoparticles on the electrical characteristic of the bottom-gate SiNW FET examined in this study [17]. To simplify the simulation, we considered a thin Pd layer, which was defined to be in a floating state to describe the role of Pd nanoparticles on the SiNW surface. The length, width, height of the SiNW in the simulation were set to 1 μm, 70 nm, and 80 nm, respectively, to make the simulation results comparable to the experimental data. The thickness of the native oxide layer covering the SiNW was set to 3 nm, and the SiNW was assumed to be n-type doped, with $N_d = 2 \times 10^{18}/cm^3$. The simulated cross-sectional electron current density along the

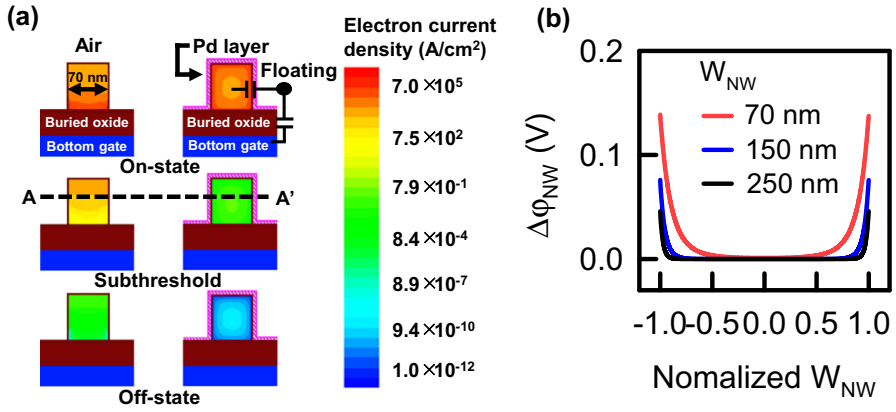

Fig. 3. (a) Simulated electron current density under various operation regimes, i.e., on-state, subthreshold, and off-state, with and without a Pd layer at V_{DS} = 50 mV. The Pd layer, with a work function of 5.1 eV, was created on the top surface and was declared as a floating state. (b) Extracted electrostatic potential $\Delta\varphi_{NW}$ inside the SiNWs versus normalized W_{NW} for various W_{NW} values. The width was normalized by its value at the surface.

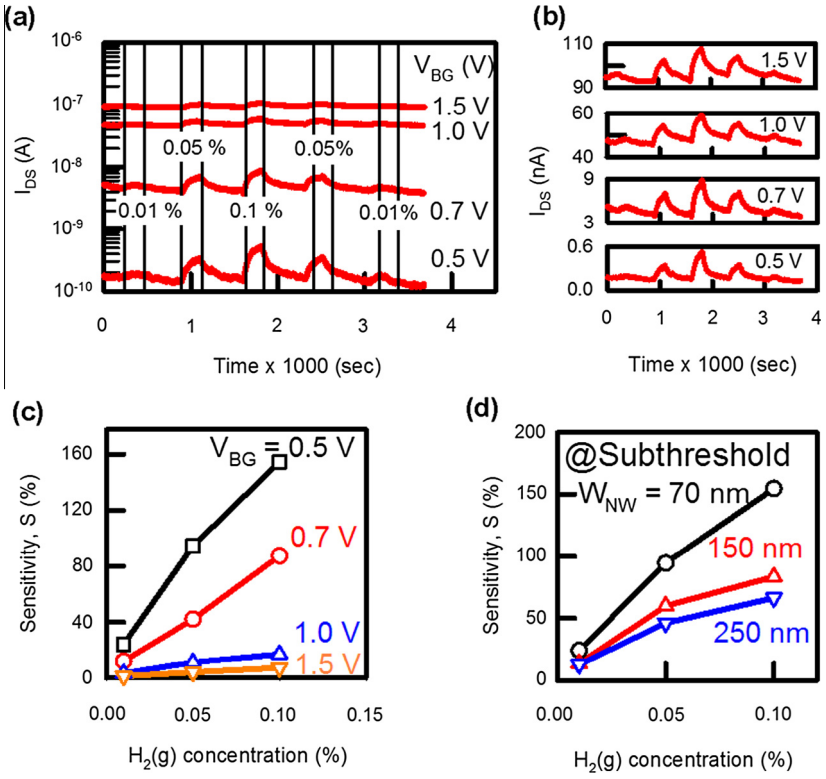

Fig. 4. The hydrogen response characteristics of the SiNW FET sensor functionalized with Pd nanoparticles. Real-time measurement of the drain current upon exposure to H_2 of different concentrations at various values of V_{BG} at V_{DS} = 50 mV on a (a) log and (b) linear scale. The sensitivity was extracted from (a) for (c) various V_{BG} and (d) W_{NW} values.

W_{NW} direction was extracted, as shown in Fig. 3(a). The results show that only electrons near the buried oxide accumulate in the on-state in the SiNW FET without a thin Pd layer. However, with the Pd layer, electrons accumulate not only near the buried oxide but also along the Pd layer because of the coupling effect between the bottom gate and Pd layer, which provides a reasonable explanation for the enhanced I_{ON}. The coupling effect can be attributed to the fact that the potential of the floating Pd layer follows the bottom gate potential, i.e., V_{BG} [14,15]. As a result, the gate control over the SiNW channel can be improved, resulting in more accumulation of electrons near the Pd layer. Although we used a continuous Pd layer in the simulation, not discrete Pd nanoparticles, we believe that the coupling effect can also be observed in discrete Pd nanoparticles because the distance between the nanoparticles is small enough to generate a strong capacitive coupling effect. Moreover, it is apparent that the electron current density in the SiNW FET with a Pd layer can be better adjusted to various operating regimes, i.e., off-state, sub-threshold, and on-state, compared to that in the SiNW FET without a Pd layer. This finding also provides evidence for the steeper SS observed in the SiNW FET with Pd nanoparticles.

It is natural to expect that the greatest enhancement in I_{ON} and SS can be achieved when a large volume of the SiNW is gated due to Pd nanoparticles. This scenario can be realized when a SiNW with a small W_{NW} is used. Fig. 3(b) shows the extracted electrostatic potential of the SiNW FETs along the A–A' direction indicated

in Fig. 3(a) for the subthreshold regime. $\Delta\varphi_{NW}$ is defined as the difference in electrostatic potential between the SiNW FETs with and without a Pd layer. For a SiNW with a large W_{NW} value of 250 nm, $\Delta\varphi_{NW}$ shows a small value at the surface of the SiNW and almost zero near the center of the SiNW. For a SiNW with a small W_{NW} value of 70 nm, however, the value of $\Delta\varphi_{NW}$ becomes large at the surface of the SiNW. Therefore, it can be concluded that the improvement of gate control over the SiNW channel is greater for smaller values of W_{NW}, which is also verified by a clear experimental evidence shown in Fig. 2(b).

4. Experimental results and discussion

Based on the foregoing analysis, we characterized the sensor response to H_2 gas and optimized the sensor performance by adjusting the operating regime of our bottom-gate SiNW FET-based sensor. For the experiment, the SiNW FET with Pd nanoparticles was mounted on a vacuum chamber probe station equipped with an electrical probing system and a gas inlet/outlet. The test H_2 gas was injected into the gas inlet by mixing dry synthetic air (79% N_2 and 21% O_2) and 0.1% H_2 gas in air, derived from gas cylinders. The concentration of the test H_2 gas was controlled by the flow rate of each gas using mass flow controllers (MFCs), while the total gas flow rate was maintained at 100 sccm. Before measuring the operation of a SiNW FET-based H_2 sensor, we filled the vacuum chamber with air gas for one hour. After an hour, the H_2 or the air gas was kept in the flowing state during the measurements. The I_{DS} of the SiNW FET-based H_2 sensor was measured in real time using an Agilent 4156C at a constant drain-to-source voltage (V_{DS}) of 50 mV and various bottom-gate voltages (Fig. 4 (a) and (b)). All experiments were performed at room temperature.

From the results obtained, we confirmed that I_{DS} increased upon the injection of the H_2 gas but decreased thereafter upon the injection of fresh air, which indicates that the operation of our devices was reversible [5]. These responses for H_2 gas can be attributed to the fact that hydrogen atoms dissociated on the surface of the Pd nanoparticles could diffuse into the Pd nanoparticles and were then absorbed onto the Pd–SiO_2 interface on top of the SiNW channel. These hydrogen atoms were then polarized and gave rise to a positive dipole layer, which correspondingly caused an increase in I_{DS} by attracting more electrons flowing through the SiNW channel due to an additional gating effect [10]. Moreover, it was observed that as the concentration of H_2 gas was increased from 0.01% to 0.1%, the change of I_{DS} also increased.

To investigate the performance of the sensor in different operating regimes, we performed the H_2 gas-sensing experiment at various bottom-gate voltages. It should be noted that although the change in I_{DS} in response to the concentration of H_2 gas was directly measured in the sensing experiments, the value depends on the properties of individual SiNWs and thus does not reflect intrinsic sensitivity. Therefore, we introduced the sensitivity parameter $S = (I_{H2} - I_{Air})/I_{Air} \times 100$ (%), where I_{H2} and I_{Air} are the I_{DS} of SiNW FETs functionalized by Pd nanoparticles in H_2 gas and in air, respectively. Fig. 4(c) shows the sensitivity toward H_2 gas at various bottom-gate voltages. For a H_2 gas concentration of 0.1%, the sensitivity reached 154.5% at $V_{BG} = 0.5$ V and was reduced to 7.5% at $V_{BG} = 1.5$ V. Although the absolute change in I_{DS} was greater at $V_{BG} = 1.5$ V, a more distinct signal was observed at $V_{BG} = 0.5$ V; in the latter condition, the SiNW FET with Pd nanoparticles was in the subthreshold regime, in which I_{DS} was exponentially changed by the V_{BG}, as previously shown in Fig. 2 (b) [9]. Therefore, we can conclude that understanding the electrostatic behavior of SiNW FET-based H_2 sensors containing Pd nanoparticles would be crucial and helpful in optimizing the sensor performance. We further analyzed the H_2 responses of the SiNW FET containing Pd nanoparticles in the subthreshold regime for various values of W_{NW} (Fig. 4(d)). It is also concluded that the SiNW FET with Pd nanoparticles could exhibit much higher sensitivity toward H_2 gas with a small value of W_{NW} due to the reduced dimensions and higher surface/volume ratio.

5. Summary

In summary, we demonstrated that the electrostatic properties of a SiNW FET-based H_2 sensor could be significantly altered by the deposition of Pd nanoparticles on the SiNW surface. It was observed that the electrostatic potential of Pd nanoparticles deposited on the SiNW surface could be coupled to the bottom-gate voltage, resulting in a significant enhancement in the electrical properties of the SiNW FET. Both the SS and I_{ON} values of the SiNW FET were improved by the deposition of Pd nanoparticles, which became apparent when a SiNW with a small W_{NW} value was used in the channel. Based on these results, we could adjust the operating regimes of SiNW FET-based H_2 sensors by controlling the V_{BG} and obtain high sensitivity toward H_2 gas in the subthreshold regime. Therefore, we expect that our analysis will enable the efficient design of sensors based on SiNW FETs with a bottom-gate structure.

Acknowledgements

This work was supported by the National Research Foundation of Korea (NRF) Grant funded by the Korea Government (Ministry of Education, Science and Technology, MEST) (Nos. 2014064116 and 2014028058) and BK21+ (Educational Research Team for Creative Engineers on Material-Device-Circuit Co-Design). The CAD software was supported by SYNOPSYS and IDEC.

References

[1] Cui Y, Wei Q, Park H, Lieber CM. Nanowire nanosensors for highly sensitive and selective detection of biological and chemical species. Science 2001;293 (5533):1289–92.
[2] Stern E, Klemix JF, Routenberg DA, Wyrembak PN, Turner-Evans DB, Hamilton AD, et al. Label-free immunodetection with CMOS-compatible semiconductor nanowires. Nature 2007;445(7127):519–22.
[3] Li Z, Chen Y, Li X, Kamins TI, Nauka K, Williams RS. Sequence-specific label-free DNA sensors based on silicon nanowires. Nano Lett 2004;4(2):245–7.
[4] Kamins TI, Sharma S, Yasseri AA, Li Z, Straznicky J. Metal-catalysed, bridging nanowires as vapour sensors and concept for their use in a sensor system. Nanotechnology 2006;17(11):S291.
[5] Chen ZH, Jie JS, Luo LB, Wang H, Lee CS, Lee ST. Applications of silicon nanowires functionalized with palladium nanoparticles in hydrogen sensors. Nanotechnology 2007;18(34):345502.
[6] Skucha K, Fan Z, Jeon K, Javey A, Boser B. Palladium/silicon nanowire Schottky barrier-based hydrogen sensors. Sens Actuators B 2010;145(1):232–8.
[7] Chen X, Wong CK, Yuan CA, Zhang G. Nanowire-based gas sensor. Sens Actuators B 2013;177:178–95.
[8] Park I, Li Z, Pisano AP, Williams RS. Top-down fabricated silicon nanowire sensors for real-time chemical detection. Nanotechnology 2010;21(1):015501.
[9] Gao XPA, Zheng G, Lieber CM. Subthreshold regime has the optimal sensitivity for nanowire FET biosensors. Nano Lett 2009;10(2):547–52.
[10] Hubert T, Boon-Brett L, Black G, Banach U. Hydrogen sensors – a review. Sens Actuators B 2011;157(2):329–52.
[11] Cao A, Sudholter EJ, de Smet LC. Silicon nanowire-based devices for gas-phase sensing. Sensors 2013;14(1):245–71.
[12] Lee J, Lee J-M, Lee JH, Lee WH, Uhm M, Park B-G, et al. Complementary silicon nanowire hydrogen ion sensor with high sensitivity and voltage output. IEEE Electron Device Lett 2012;33(12):1768–70.
[13] Nah J, Kumar SB, Fang H, Chen Y-Z, Plis E, Chueh Y-L, et al. Quantum size effects on the chemical sensing performance of two-dimensional semiconductors. J Phys Chem C 2012;116(17):9750–4.
[14] Jang H, Lee J, Lee JH, Seo S, Park B-G, Kim DM, et al. Analysis of hysteresis characteristics of silicon nanowire biosensors in aqueous environment. Appl Phys Lett 2014;99(25):252103.
[15] Chen S, Zhang S-L. Gate coupling and carrier distribution in silicon nanowire/nanoribbon transistors operated in electrolyte. J Vac Sci Technol A 2011;29(1):011022.
[16] Tu R, Zhang L, Nishi Y, Dai H. Measuring the capacitance of individual semiconductor nanowires for carrier mobility assessment. Nano Lett 2007;7 (6):1561–5.
[17] Sentaurus User's Manual. Mountain View (CA): Synopsys, Inc.; 2013.